The International Journal of Advanced Manufacturing Technology (2018) 99:737–746
https://doi.org/10.1007/s00170-018-2498-4

ORIGINAL ARTICLE

Effect of symmetrical conical micro-grooved texture on tool–chip friction property of WC-TiC/Co cemented carbide tools

Minghua Pang[1] · Yongfang Nie[1] · Lijie Ma[1]

Received: 13 April 2018 / Accepted: 20 July 2018 / Published online: 10 August 2018

Abstract

Surface texturing has been an attracting interest in metal cutting fields because of their tribological improvement at the tool–chip interface. A novel symmetric conical micro-grooved texture (S-5) was proposed and manufactured on the tool rake face using laser texture technology. The improvement effect of surface texturing (S-5) on tool–chip friction property was tested with AISI 1045 steel cutting experiment for various cutting speeds (80 to 160 m/min) under flood lubrication condition. Meanwhile, cutting performance of S-5 were evaluated against parallel micro-grooved texture tools (P-0) for a better clarification of the interaction mechanism. Experimental results indicated that surface texturing (P-0, S-5) on tool rake face all successfully resulted in a reduced cutting force, tool–chip friction coefficient, and tool surface wear than conventional tools (C-0). Moreover, S-5 showed a more obvious advantage in the improvement of tool–chip interfacial friction property than P-0.When cutting speed was smaller than 120 m/min, the friction coefficient obtained with the conventional (C-0) and textured tools (P-0, S-5) all showed a downward trend, and a smallest friction coefficient was appeared for S-5. When the cutting speed was greater than 120 m/min, an upward trend of friction coefficient was obtained for the C-0 and P-0 tools. However, a downward trend of friction coefficient was still existed for S-5. Detailed research indicated that the symmetric conical micro-grooved texture on the tool rake face could accelerate the infiltration speed of cutting fluid at the tool–chip interface. More cutting fluid would be supplied and stored at the tool–chip interface. So, symmetric conical micro-grooved texture on the tool rake face had a best lubrication effect of cutting fluid than conventional (C-0) and parallel micro-grooved texture tools (P-0).

Keywords Symmetrical conical micro-grooved texture · Tool–chip friction · WC-TiC/Co cemented carbide · Surface texturing

NomenclatureCutting tools

C-0	Conventional tools
P-0	Parallel micro-grooved texture tools
S-5	Symmetrical conical micro-grooved texture tools

Textured parameters

H	Textured zone height on the tool rake face (mm)
W	Textured zone width on the tool rake face (mm)
L	Distance of textured elements (mm)
d	Small end dimension of textured elements (μm)
D	Dig end dimension of textured elements (μm)
h	Texture depth (μm)
α	Conical angle of textured elements (°)
δ	Distance of textured zone to main cutting edge (°)
β	Symmetric angle of textured zone (°)

Cutting conditions

v	Cutting speed (m/min)
α_p	Depth of cut (mm)
f	Feed rate (mm/rev)
γ_0	Rake angle (°)
ϕ	Shear angle of the chip (°)
F_x	Radial thrust force (N)
F_y	Axial force (N)
F_z	Main cutting force (N)
τ_s	Shearing strength of workpiece material (MPa)
A_s	Adhesion area of tool–chip (mm^2)
τ_m	Shearing strength of lubrication layer (MPa)
A_m	Action area of the lubrication layer (mm^2)
A	Total contact area of tool–chip (mm^2)

✉ Minghua Pang
pangminghua909@163.com

[1] School of Mechanical and Electrical Engineering, Henan Institute of Science and Technology, Xinxiang, China

1 Introduction

Severe friction at the tool–chip interface causes high contact pressure and a large amount of cutting heat and reduces the service life of cemented carbide tools in the metal cutting process. The improvement of friction is of fundamental importance to the efficiency of the metal removal process and the tool life [1–4]. Cutting fluid is extensively used to reduce tool–chip interface friction in the metal-cutting process. Corresponding research results indicate that introducing a lubricant into the tool–chip interface can significantly reduce the friction of tools and improve the tool cutting performance [5–8]. Owing to the high normal stresses, cutting fluid infiltration into the tool–chip interface only occurs at the rear portion of the contact area which limits the lubrication effect of the cutting fluid [5, 8].

In recent years, surface texturing technology was proposed [6, 9]. Surface texturing, which refers to appropriately structuring the topography of a functional surface, has been extensively used in many fields. Moreover, all of the experimental results indicate that the surface texture can trap wear debris [10, 11], store lubricant [12, 13], and increase the load-carrying capacity of a sliding interface under a fluid lubrication condition [14–16]. So, surface texture is introduced into the tool surface to improve lubrication and decrease friction at the tool–chip interface. Corresponding research results indicate that the surface texture on the tool surface decrease cutting force and tool–chip friction [17, 18]. This significant potential has led to increasing attempts to clarify the effect of tool surface texturing on the friction property of the tool–chip interface. For example, Koshy et al. [19] fabricated discrete grooves and area texture on the rake face of T-15 inserts. Experimental results indicated that surface texturing on the tool rake face could bring about a significant reduction in machining force, and area texture had a more noticeable effectiveness than discrete groove texture. Enomoto et al. [20, 21] investigated the effect of micro/nano-grooves on anti-adhesive properties of the tools in aluminum alloy milling tests. Experimental results showed that micro/nano-grooves parallel to the main cutting edge significantly improved the anti-adhesive properties of the tools in wet cutting condition. The main reason was the improvement of cutting fluid storing and providing ability at the tool–chip interface. Obikawa et al. [22] investigated the effect of textured type (grooves perpendicular/parallel to the cutting edge and matrix of square pits/dots) on tool cutting performance in aluminum alloy cutting test under water-immiscible cutting oil lubrication condition. It was found that lubricant fill into the tool–chip interface was improved by tool surface texturing, and parallel grooves and square-dot type of micro-textures were more effective in this aspect. For further clarifying the effectiveness of cutting fluid lubrication conditions on textured tool cutting performance, Zhang et al. [23] investigated the correlation between tool surface texture and lubrication condition in AISI 1045-hardened steel cutting tests. Experimental results showed that the cutting performance of textured tools was affected by lubrication condition, and a more noticeable cutting performance was obtained for textured tools under full lubrication condition.

In the present study, a new symmetric conical micro-grooved texture was proposed and fabricated on the tool rake face using laser texture technology. The effectiveness of symmetric conical micro-grooved texture on the tool cutting force, tool–chip friction coefficient, and tools surface wear were studied and compared with parallel micro-grooved texture tools.

2 Experimental details

2.1 Development of cutting tool with surface texturing

WC-TiC/Co-cemented carbide inserts (YT15, ISO P10-type) were selected as the cutting tool material in this study. The composition and mechanical properties of this tool material are listed in Table 1. The size of the cutting inserts are 16 mm × 16 mm × 5 mm, and the average surface roughness is 0.02 μm. Laser texture technology has been a competitive technique for fabricating surface texture on the tool rake face [17, 18]. A fiber laser engraving machine (YLP-F10, Shenzhen Han Clan Laser Technology Co., Ltd., China) was selected and used to fabricate micro-texture on the tool rake face (Fig. 1a, b). The parameters of this machine are listed in Table 2. The processing parameters of micro-texture were set as follows: output power of 3.0 W, texturing speed of 270 mm/s, texturing times of 3, and repetition frequency of 20 kHz. Corresponding research results have indicated that conical micro-channel has the directional motion characteristics of liquid [24, 25]. Surface texturing on the tool rake face can improve the infiltration of cutting fluid at interface, the

Table 1 Chemical composition and mechanical properties of the tool material

Composition (wt%)	Density (g/cm^3)	Hardness (HRA)	Flexural strength (GPa)	Yield strength (GPa)	Young's modulus (GPa)	Thermal conductivity (W/(M.°C))	Thermal expansion coefficient (10^{-6}/°C)
79% WC + 13% TiC +8% Co	11.5	91	1.15	4	525	33.5	6.51

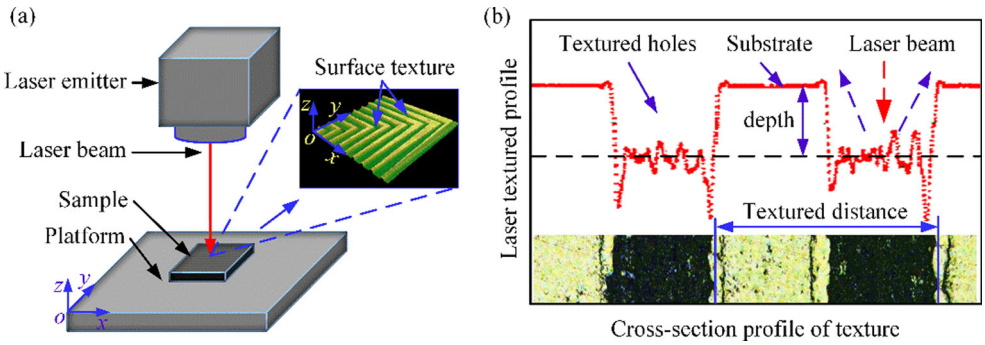

Fig. 1 **a** Schematic of laser surface texture processing and **b** cross-sectional profile of micro-grooved texture

effectiveness of which may be affected by liquid transport capacity of textured element. Inspired by this finding, a symmetric conical micro-grooved texture was speculated and fabricated on the tool rake face, and the geometrical parameters are listed in Table 3. For further clarifying the influence mechanism of symmetric conical micro-grooved texture on the tool rake face, conventional and parallel micro-grooved texture tools were selected for comparative analysis. In view of the significance of textured zone relative to the main cutting edge and the differences of corresponding research conclusions [19, 23], the average value (δ in Table 3) of 150 μm was selected in this study. After surface texturing, each sample was polished with #2000 abrasive paper to eliminate burrs, and cleaned in an ultrasonic bath with acetone for 20 min to remove residual particles. At last, the surface topography of the test samples was observed using a 3D laser scanning microscope (VK-X100K, KEYENCE Inc., Japan) to ensure that no burrs remained (Fig. 2).

2.2 Cutting tests

Cutting tests were conducted on a CA6140 lathe (CA6140, Shenyang Machine Tool Co. Ltd., China). The lathe was equipped with a commercial tool holder which had the following geometrical parameters: rake angle γ_0 of − 8°, clearance angle α_0 of 10°, inclination angle λ_s of 0°, and side cutting edge angle K_r of 42°. A dynamometer (Kistler 9257B, Kistler Co., Ltd., Switzerland) was set under the tool holder to measure the components of the cutting forces (Fig. 3a, b). The workpiece material was AISI 1045 steel with hardness of 35 HRC, the composition and mechanical properties are listed in Table 4. The form of workpiece was a round bar with a diameter of ϕ60 mm. A water-miscible cutting fluid (JAEGER SW-105, 5%) was supplied as a flood, the flow rate was 40 cc/h along the tool rake face. The cutting test parameters are listed in Table 5. The test duration of the cutting process for each sample was set as 3 min to obtain wear marks on the tool rake face. All tests were performed thrice to ensure the reproducibility of test results, and the average values and standard deviation were calculated and recorded. The morphology of worn region of the cutting tool was examined using a 3D laser scanning microscope (VK-X100K, KEYENCE Inc., Japan).

3 Results and discussion

3.1 Cutting force

Cutting force can be used to characterize tool cutting performance and tool–chip interfacial friction condition [1–4]. Therefore, three components of cutting force were recorded and analyzed. Figure 4a–c depicts the average cutting forces of the conventional (C-0) and textured (P-0 and S-5) tools at different cutting speeds (80~160 m/min). As shown in Fig. 4a–c, texture on the tool rake face reduced the cutting forces (Fx, Fy, and Fz) than conventional tools (C-0). Moreover, the symmetric conical micro-grooved tools (S-5) showed a more noticeable effectiveness in this aspect than the parallel micro-grooved texture tools (P-0). The average cutting forces of the C-0 tools were 89.9 N (Fx), 115.7 N (Fy), and 141.6 N (Fz) at a cutting speed of 80 m/min, those of P-0 tools were 74.49 N (Fx), 103.8 N (Fy), and 139.5 N (Fz), and whereas those of S-5 tools were 68.28 N (Fx), 100.21 N (Fy), and 135.9 N (Fz) at the same cutting speed condition. Compared with the average cutting forces of the conventional tools (C-0), those of the P-0 tools were lower by 17.1% in Fx, 10.28% in Fy, and 1.5% in Fz, and whereas those of S-5 tools were lower by 24% in Fx, 13.4% in Fy, and 4% in Fz. These results indicated that

Table 2 Parameters of the fiber laser engraving machine

Power (W)	Scanning speed (mm/s)	Reposition precision (mm)	Wavelength (μm)	Frequency (kHz)	Laser spot diameter (mm)	Laser type	Pulse–width (ns)	Single-pulse energy (mj)
10	≤ 9000	± 0.001	1.06	20	0.015	IPG	100	1

Table 3 Geometrical parameters of the symmetric conical micro-grooved texture on the tool rake face

Textured type	Geometrical parameters	Value		
		Conventional tool (C-0)	Parallel micro-grooved texture (P-0)	Symmetrical conical micro-grooved texture (S-5)
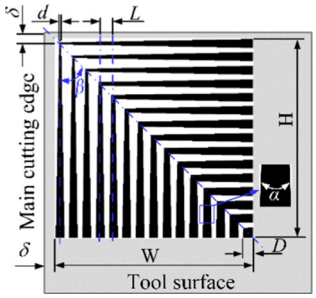	H /mm	-	5	5
	W /mm	-	5	5
	L /mm	-	0.34	0.34
	d /μm	-	40	40
	D /μm	-	40	477
	h /μm	-	25	25
	α /°	-	0	5
	δ /μm	-	150	150
Geometry parameter model of surface texturing	β /°	-	90	45

symmetric conical micro-grooved texture on the tool rake face had the best effect on cutting force reduction under flood lubrication condition. In view of previous conclusions, texture on the tool rake face can affect the infiltration and storage of cutting fluid at the tool–chip interface [17–20, 23]. And more cutting fluid infiltration and storage could reduce the cutting force of tools [19, 20, 23]. Thus, the symmetric conical micro-grooved texture on the tool rake face should have a more noticeable advantage in the infiltration and storage of cutting fluid than C-0 and P-0 tools. In addition, tool cutting forces

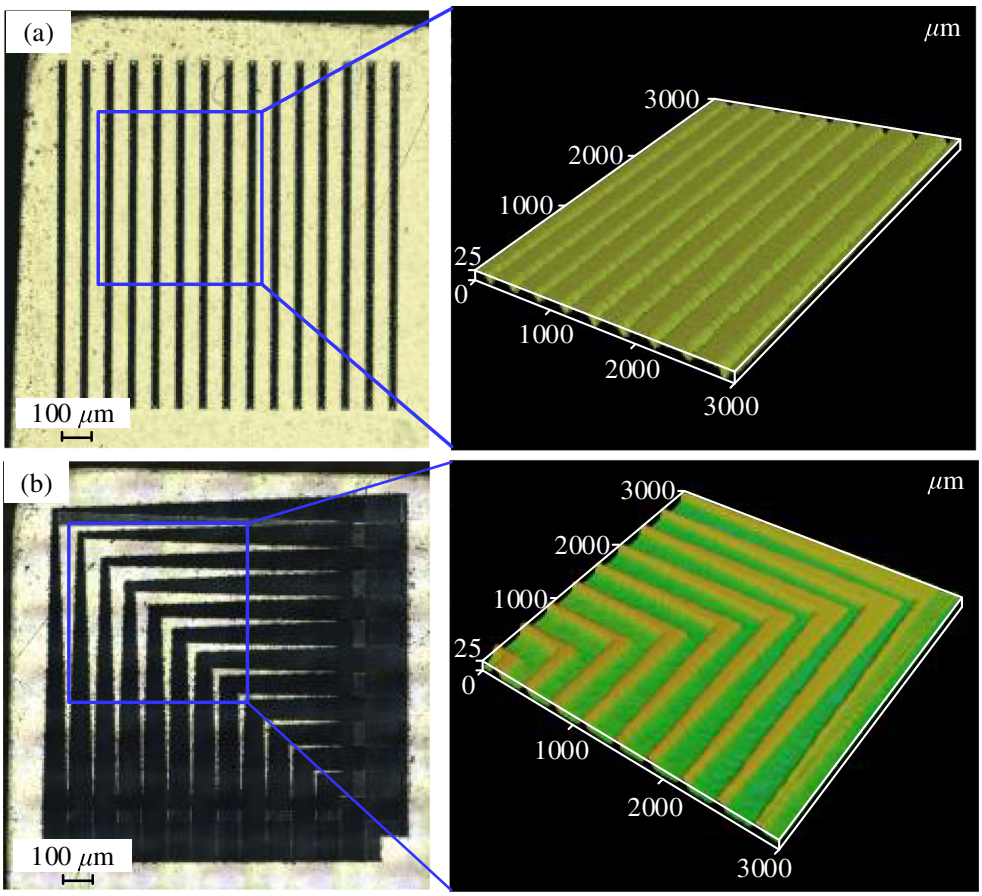

Fig. 2 Cutting tools with **a** parallel micro-grooved texture (P-0), **b** symmetrical conical micro-grooved texture (S-5), and local 3D topography of surface texturing

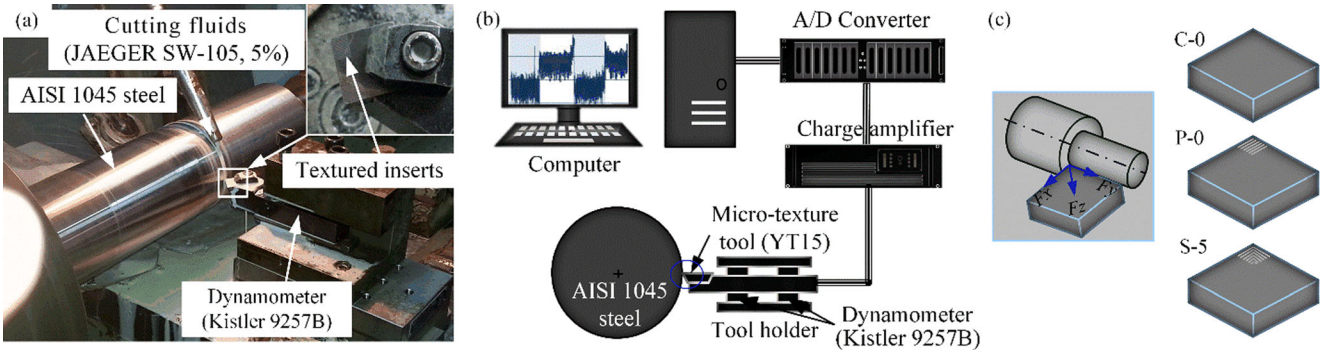

Fig. 3 **a** Cutting experimental setup, **b** schematic diagram, and **c** conventional and textured cutting tools

firstly increased and then followed a downward trend with the increase of cutting speed as shown in Fig. 4a–c. These results indicated that the softened effect of workpiece material induced by cutting heat was existing in tool cutting experiment [23, 26]. In addition, the cutting force difference of the C-0, P-0, and S-5 tools increased with the increase of cutting speed (Fig. 4d–f). The main reason was that cutting fluid already infiltrated at the tool–chip interface that would be taken away by the chips and evaporated by cutting heat, and the mount of cutting fluid taken away by chips and evaporated by cutting heat would increase with the increase of cutting speed [23]. In this case, the increase of cutting fluid infiltration at interface had a directly effect on interfacial lubrication condition. Surface texture on the tool rake face can increase the infiltration of cutting fluid at the tool–chip interface [17–20, 23]. And S-5 tools exhibited a more noticeable advantage in cutting force reduction than the P-0 tools at high cutting speeds. Thus, symmetric conical micro-grooved texture must had a more obvious advantage in cutting fluid infiltration and storage at the tool–chip interface. Accordingly, the transportation velocity of cutting fluid at the tool–chip interface should be accelerated by symmetric conical micro-grooved texture element [24, 25].

3.2 Friction coefficient at the tool–chip interface

Friction at the tool–chip interface exerts a critical effect on metal-cutting efficiency and tool life and has become a key subject in machining research [1–3]. Friction coefficient is the characteristic parameter of the interfacial friction condition. Therefore, the average friction coefficient at the tool–chip interface was calculated according to the following formulas [27]:

$$(\beta - \gamma_0) = \tan^{-1}\left(\frac{F_y}{F_z}\right) \tag{1}$$

$$\varphi + \beta - \gamma_0 = \frac{\pi}{4} \tag{2}$$

$$\mu = \tan(\beta) \tag{3}$$

$$F = \sqrt{F_x^2 + F_y^2 + F_z^2} \tag{4}$$

where β is the friction angle, γ_0 is the rake angle, φ is the shear angle of the chip, F_x is the radial thrust force, F_y is the axial force, and F_z is the main cutting force.

Figure 5a presents the detailed values of the friction coefficient of three types of cutting tools (C-0, P-0, and S-5) at the tool–chip interface under flood lubrication condition. As shown in Fig. 5a, a smaller friction coefficient was obtained with textured tools (P-0 and S-5) than conventional ones (C-0). These results indicated that the texture on the tool rake face improved the tool–chip interface friction, and S-5 tools showed a more obvious advantage in this aspect than P-0 tools. The lubrication of cutting fluid at the tool–chip interface play an important role in the interfacial friction. The increase of cutting fluid infiltration can reduce the interfacial coefficient. In view of previous conclusions, texture on the tool rake face can change the infiltration and storage of cutting fluid at the tool–chip interface [17–20, 23]. Thereby, the differences in the friction coefficient reduction between P-0 and S-5 tools

Table 4 Chemical composition and properties of the AISI 1045 steel

Composition (wt%)	C	Si	Mn	Cr	Ni	Cu	P	S
	0.42–0.5	0.17–0.37	0.5–0.8	≤0.25	≤0.25	≤0.25	≤0.035	≤0.035
Properties	Density (g/cm^3)	Hardness (HRC)	Young's modulus (GPa)	Poisson's ratio	Tensile strength (MPa)	Yield strength (MPa)	Extension rate (%)	Section shrinkage (%)
	7.85	35	210	0.3	600	355	≥16	≥40%

Table 5 Cutting test parameters

Cutting parameters	Detailed value				
Cutting speed v/m/min	80	100	120	140	160
Depth of cut α_p/mm	0.5	0.5	0.5	0.5	0.5
Feed rate f/mm/rev	0.1	0.1	0.1	0.1	0.1

were the effectiveness of surface texture on the infiltration and storage of cutting fluid at the tool–chip interface.

In addition, the friction coefficient obtained with the conventional and textured tools firstly decreased and then increased with the increase of cutting speed (Fig. 5a, b). The main reason was that the cutting fluid obtained at the tool–chip interface was sufficient when cutting speed was small [23]. At the same time, the cutting temperature at interface increased with the increase of cutting speed which soften the interfacial material [23, 26]. Thereby, the friction coefficient of tool–chip interface decreased with the increase of cutting speed. With the further increase of cutting speed, cutting fluid already infiltrated the tool–chip interface that would be taken away by the chips. Meantime, more cutting fluid was heated and evaporated by cutting heat. The lubrication of the cutting fluid at the tool–chip interface would be weakened with the increase of cutting speed [23]. So, an upward trend of friction coefficient was obtained for the C-0 and P-0 tools. However, a

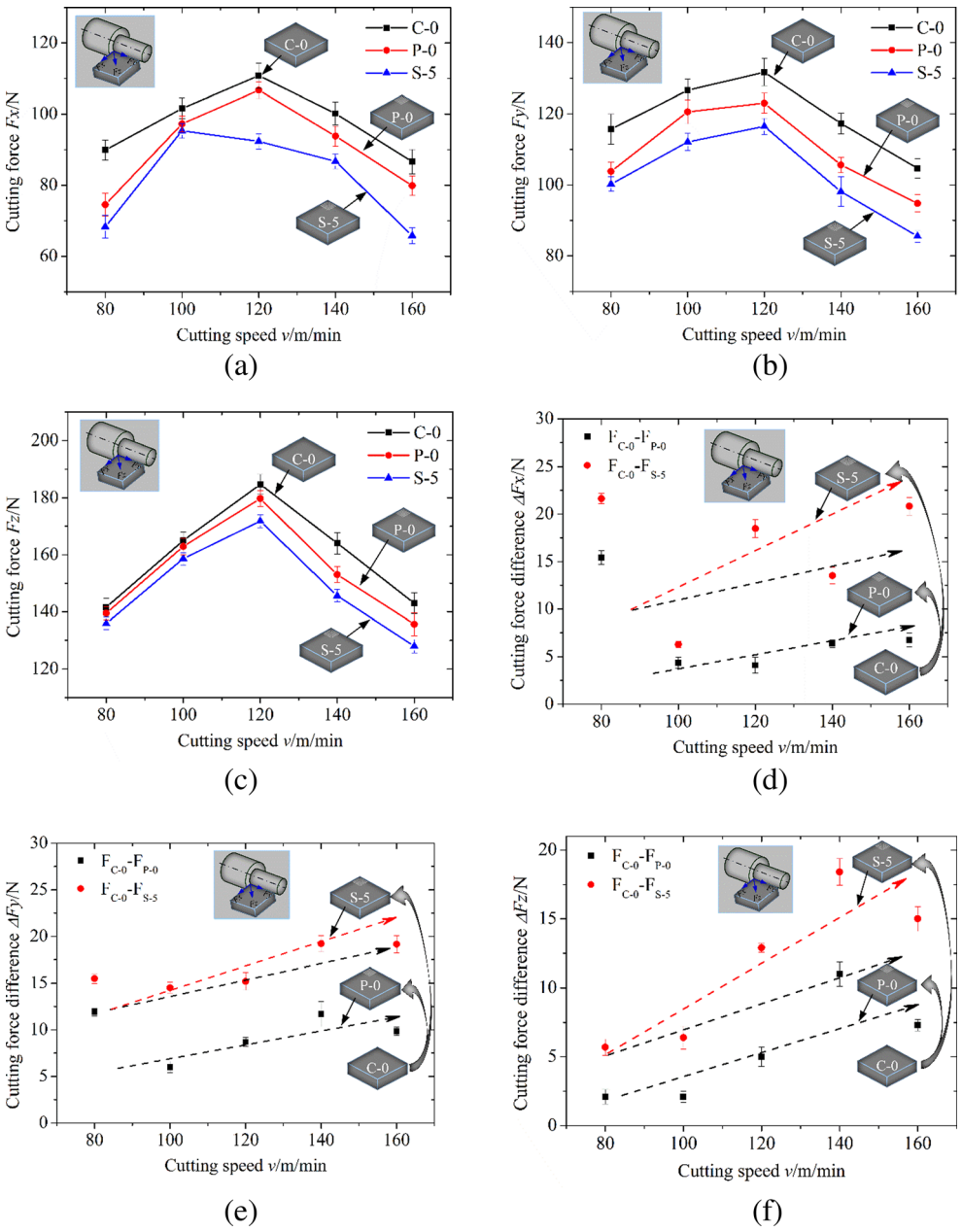

Fig. 4 Three components of cutting forces of the conventional (**a**) and textured tools (**b**, **c**) at the different cutting speed, and the cutting force difference (**d**–**f**)

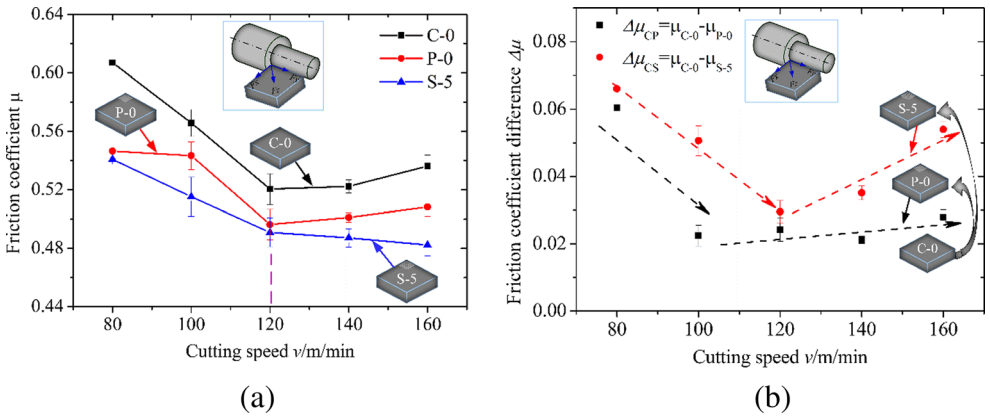

Fig. 5 The detailed friction coefficient at the tool–chip interface for conventional (C-0) and textured (P-0 and S-5) tools at different cutting speeds (**a**) and the difference of friction coefficient (**b**)

downward trend of friction coefficient was still obtained with S-5 tools. And, the difference of the friction coefficients between the P-0 and S-5 tools increased with the increase of cutting speed (Fig. 5a, b). These results also indicated that the transportation velocity of cutting fluid at the tool–chip interface was accelerated by symmetric conical micro-grooved texture which quickly supplemented the loss of cutting fluid at interface.

3.3 Tool wear at the rake face

Tool life is usually evaluated on the basis of the wear of the tool surface [1–3]. In addition, tool surface wear was another evaluating indicator of tool–chip interfacial friction condition. So, the wear micrograph on the tool rake face was obtained with an optical microscope (VK-X100K, KEYENCE Inc., Japan). Figure 6a–c presents the wear micrograph of the C-0, P-0, and S-5 tools at a cutting speed of 80 m/min. A large amount of plows can be observed on the rake face of the conventional (C-0) and textured (P-0 and S-5) tools obviously. However, comparison of Fig. 6a–c indicated that a light wear mark on the textured tool surface (P-0 and S-5) was observed. In addition, the tool–chip interface contact length was also reduced by tool surface texturing. These results indicated that the friction and wear at the tool–chip interface was improved by the texture on the tool rake face under flood lubrication condition. In consideration of random inhomogeneity of tool-worn surfaces, accurate quantization of tool wear surface is difficult just from these micrographs [28]. So a single plane estimation of tool wear degree is obtained and shown in Fig.

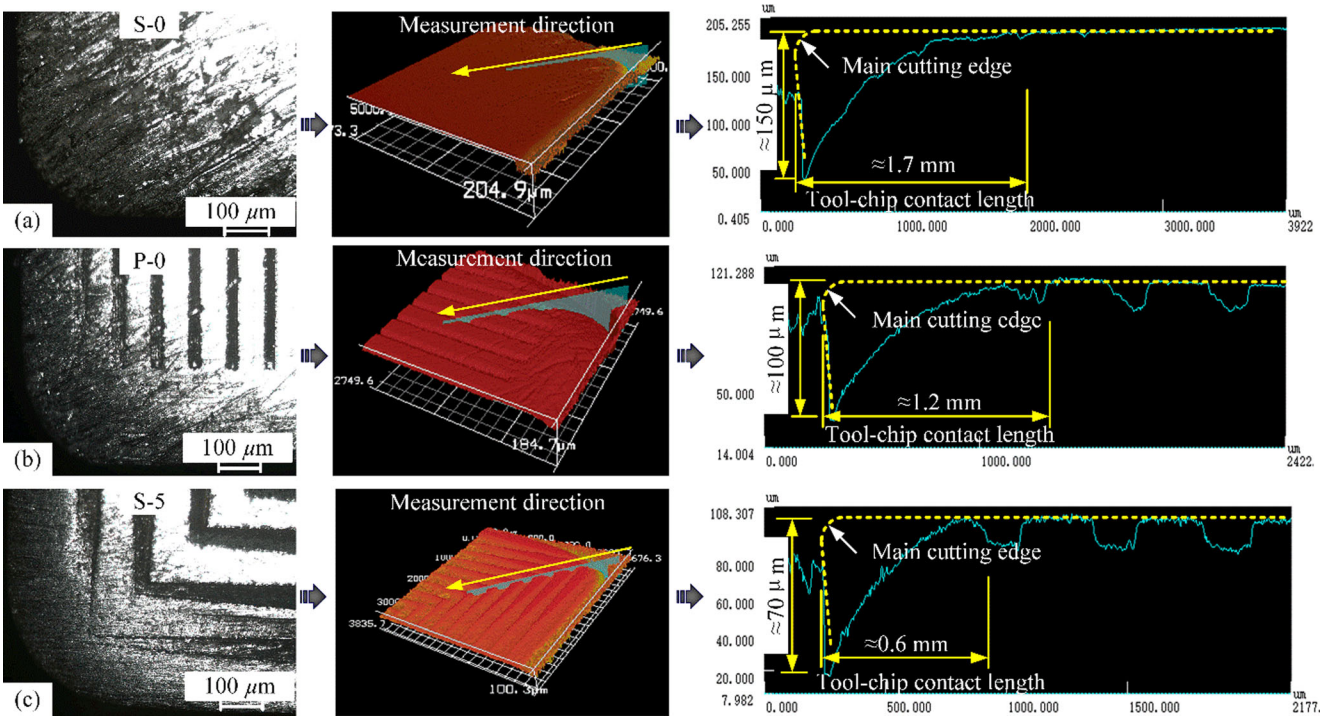

Fig. 6 Wear micrographs on the tool rake face of the conventional (C-0) (**a**) and textured tools (P-0 and S-5) (**b**, **c**) after cutting 3 min at speeds of 80 m/min

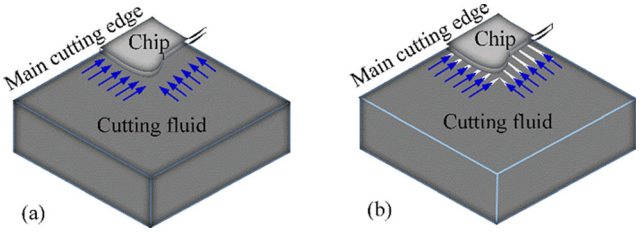

Fig. 7 Infiltration schematic of the cutting fluids at the tool–chip interface for **a** conventional tools and **b** textured tools

6b, c. Comparison of Fig. 6b, c indicated that wear degree and range were different for the P-0 and S-5 tools. The tool–chip contact length of P-0 tools was 1.2 mm and those of S-5 tools was 0.6 mm. Furthermore, the wear depth of P-0 tools was 100 μm and those of S-5 tools was 70 μm. All these results indicated that the wear mark and range of the symmetric conical micro-grooved texture tools (S-5) were all less than that of the parallel micro-grooved texture tools (P-0). Previous research results have indicated that the textures on the tool rake surface infiltrated and stored more cutting fluid than no-textured surface which improved the tribological behaviors of the tool–chip interface under cutting fluid environment [17–20, 23]. This trend was due to the increase of cutting fluid infiltration at the tool–chip interface which improved interfacial lubrication and reduced the wear mark of the tool surface [19, 23]. Figure 6 also illustrated that the infiltration of cutting fluid at the tool–chip interface was further improved by the symmetric micro-grooved texture than parallel micro-grooved texture.

4 Discussion

For further improving the tool wear, a new symmetric conical micro-grooved texture (S-5) was proposed and fabricated on the tool rake face. Cutting test of AISI 1045 steel indicated that texture on the tool rake face reduced cutting force, tool–chip friction, and tool wear under blood lubrication condition. Moreover, the symmetric conical micro-grooved texture (S-5) showed a more obvious advantage in improving the interfacial friction characteristics than parallel micro-grooved texture (P-0). Existing research results have shown that the infiltration of cutting fluid at the tool–chip interface have a direct effect on the interfacial lubrication and friction [19, 23]. And texture on the tool rake face could improve the infiltration and storage of cutting fluid at the tool–chip interface [17–20, 23]. For conventional tools, the tool–chip interface is tight solid contact during the turning process, and the lubricating fluids cannot find micro-channel into the tool–chip interface even under flood lubrication conditions [5, 23, 29]. For textured tools, a large number of micro-grooves are existed at interface, and lubricating fluids can easily filter into the contact interface, as shown in Fig. 7. In our study, parallel micro-grooved texture (P-0) on the tool rake face reduced cutting force, tool–chip friction coefficient, and tool surface wear. More importantly, symmetric conical micro-grooved texture on the tool rake face showed a more noticeable advantage in these aspects than parallel micro-grooved texture. In view of the analyses above and existing research results [17–20, 23], symmetric conical micro-grooved texture must have a more noticeable advantage in improving the infiltration and lubrication of cutting fluid at interface than parallel micro-grooved texture especially at a high cutting speed (Fig. 5a, b).

In addition, in tool cutting process, the cutting fluid that have already infiltrated the tool–chip interface would be taken away by the chips and simultaneously evaporated by the cutting heat, especially at a high cutting speed [23]. The infiltration speed of cutting fluid at the tool–chip interface have a direct influence on the interfacial lubrication condition. Essentially, the infiltration of cutting fluid at interface is the flowing of cutting fluid in micro-grooved element [5, 29]. In this case, the flowing speed of cutting fluid in micro-grooved

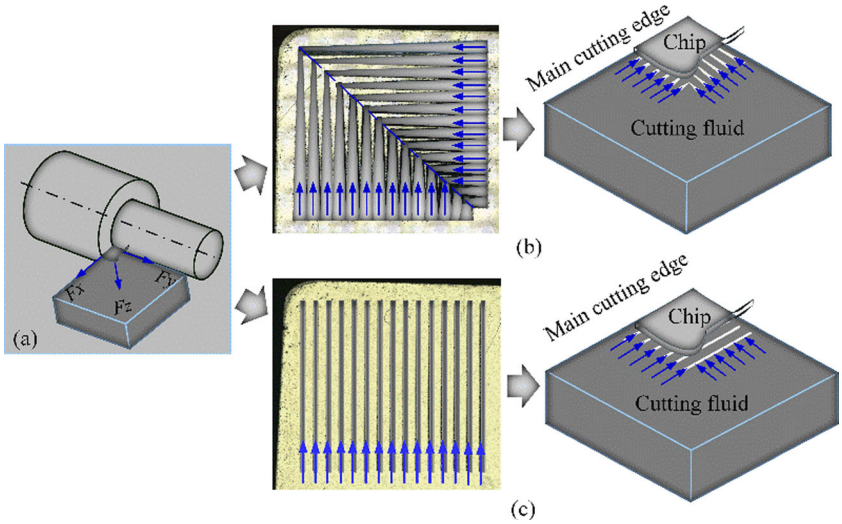

Fig. 8 **a** Metal cutting model, **b** cutting fluids infiltration in symmetric conical micro-grooved element, and **c** parallel micro-grooved element

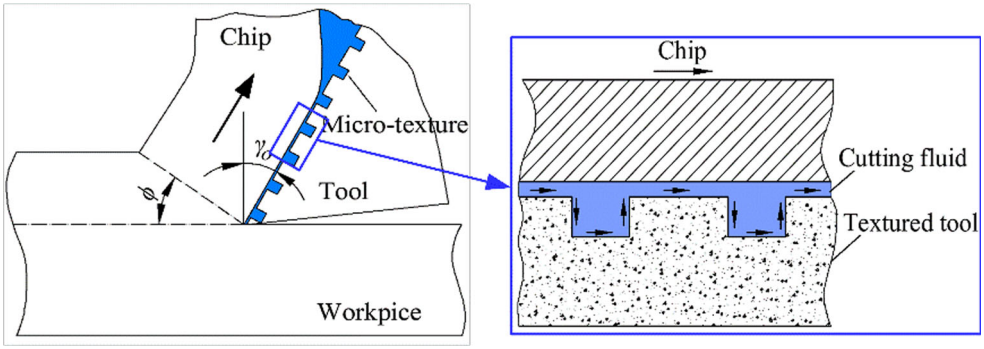

Fig. 9 Schematic of the lubrication film formation at the tool–chip interface

element was a crude evaluating indicator of surface texture effect. The flowing of cutting fluid in parallel micro-grooved element was only derived by capillary force. But, the liquid inside the conical micro-grooved channel would be driven by the combined action of surface tension gradient and capillary force which increased the flow speed of liquid [24, 25]. Thus, the infiltration speed of cutting fluid at the tool–chip interface would be accelerated by the conical micro-grooved texture. More cutting fluid would be supplied and stored at the tool–chip interface than conventional and parallel micro-grooved texture tools. However, this characteristic of tool surface texture has not been reported for other texture types in related literatures so far. For these reasons, the symmetric conical micro-grooved texture on the tool rake face showed a more obvious advantage in improving the infiltration and lubrication of cutting fluid than conventional and parallel micro-grooved texture tools.

The infiltrated cutting fluid formed a firm lubrication film by physical and chemical adsorption at the tool–chip interface (Figs. 8 and 9) [5, 29]. Although there is an existence of lubrication at interface, obvious sliding marks were observed on the tool rake face (Fig. 6b, c). These results indicated that the tool–chip interface was in boundary lubrication condition. So the interfacial frictional force could be calculated as [30].

$$F_f = \tau_s A_s + \tau_m A_m, \tag{5}$$

where τ_s is the shearing strength of the workpiece material, A_s is the adhesion area between the tool rake face and the chip, τ_m is the shearing strength of the lubrication layer, A_m is the action area of the lubrication layer, and A is the total contact area between the tool rake face and the chip.

The interfacial friction force have two parts, the shear strength of solid contact area between the tool rake face and the chip and lubrication layer of cutting fluid according to Eq. (5). The infiltration of the cutting fluid at the tool–chip interface could lead to a reduction in the solid contact area. Obviously, the shear strength of cutting fluid was smaller than the AISI 1045 steel. So a smaller interfacial friction would be obtained with the increase in cutting fluid infiltration. To summarize, texture on the tool rake face improve the infiltration and lubrication of cutting fluid at interface, then reduce the tool–chip friction, tool surface wear, and cutting force. Moreover, symmetric conical micro-grooved texture has a more noticeable advantage in cutting fluid infiltration speed than parallel micro-grooved texture. Then the smallest friction coefficient, tool surface wear, and cutting force were obtained in tool cutting process.

5 Conclusions

In this study, a new symmetric conical micro-grooved texture was proposed and manufactured on the tool rake face with laser texture method. Cutting tests of AISI 1045 steel were conducted with the textured and conventional tools at different cutting speeds under flood lubrication condition. Experimental results showed that the presence of texture on the tool rake face decreased the cutting force, tool–chip friction coefficient, and tool surface wear. Moreover, symmetric conical micro-grooved texture on the tool rake face has a more noticeable advantage in these aspects than parallel micro-grooved texture. The findings based on the analytical results were as follows:

(1) Texture on the tool rake face effectively improved the infiltration and lubrication of cutting fluid at the tool–chip interface. Hence, the cutting forces, average friction coefficient, and tool wear of textured tools were decreased effectively compared with those of conventional tools.
(2) Symmetric conical micro-grooved texture had a more obvious advantage in improving cutting fluid infiltration and storage at tool–chip interface. So, S-5 showed a more obvious advantage in the improvement of tool–chip interfacial friction property than P-0. When cutting speed was smaller than 120 m/min, the friction coefficient obtained with the textured tools (P-0 and S-5) all showed a downward trend, and a smallest friction coefficient appeared for S-5. When the cutting speed was greater than 120 m/min, an upward trend of friction coefficient was obtained for the P-0 tools. However, a downward trend of friction coefficient was still existed for S-5.

(3) The flowing speed of cutting fluid in micro-grooved element have a directly influence on the infiltration of cutting fluid, and was a crude evaluating indicator of surface texture effect. The liquid inside the conical micro-grooved channel would be driven by the combined action of surface tension gradient and capillary force. Thus, the infiltration speed of cutting fluid at the tool–chip interface would be accelerated by the symmetric conical micro-grooved texture. More cutting fluid would be supplied and stored at the tool–chip interface than conventional and parallel micro-grooved texture tools. For these reasons, the symmetric conical micro-grooved texture on the tool rake face showed a more obvious advantage in improving the tool–chip friction property under blood lubrication condition.

(4) Symmetric conical micro-grooved texture on the tool rake face has obvious advantage in improving tool–chip friction property especially at a high cutting speed condition. But, the use condition limitations of this textured type is that the effectiveness is obtained only in wet cutting condition. Moreover, optimal parameters of this textured type are not completely clarified for different workpiece materials. In our next phase of work, relevant research work will be further carried out.

Funding information This study was supported by the key scientific and technological project of Henan province (grant no. 162102210104).

Compliance with ethical standards

Conflict of interest The authors declare that they have no conflict of interest.

References

1. Astakhov VP (2006) Tribology of metal cutting, 1th edn. Elsevier, London
2. Bailey JA (1975) Friction in metal machining - mechanical aspects. Wear 31:243–275
3. Ozlu E, Budak E, Molinari A (2009) Analytical and experimental investigation of rake contact and friction behavior in metal cutting. Int J Mach Tool Manu 49:865–875
4. Kim DY, Kim DM, Park HW (2018) Predictive cutting force model for a cryogenic machining process incorporating the phase transformation of Ti-6Al-4V. Int J Adv Manuf Technol 96(1–4):1293–1304
5. Hwang J (2014) Direct observation of fluid action at the chip-tool interface in machining. Int J Precis Eng Manuf 15:2041–2049
6. Gachot C, Rosenkranz A, Hsu SM, Costa HL (2017) A critical assessment of surface texture for friction and wear improvement. Wear 372-373:21–41
7. Krolczyk GM, Nieslony P, Maruda RW, Wojciechowski S (2017) Dry cutting effect in turning of a duplex stainless steel as a key factor in clean production. J Clean Prod 142:3343–3354
8. Gariani S, Shyha I, Inam F, Huo D (2018) Experimental analysis of system parameters for minimum cutting fluid consumption when machining Ti-6Al-4V using a novel supply system. Int J Adv Manuf Technol 95(5–8):2795–2809
9. Evans CJ, Bryan JB (1999) "Structured", "textured" or "engineered" surfaces. Ann CIRP 48(2):541–556
10. Ryk G, Etsion I (2006) Testing piston rings with partial laser surface texturing for friction reduction. Wear 261:792–796
11. Kovalchenko A, Ajayi O, Erdemir A, Fenske G (2011) Friction and wear behavior of laser textured surface under lubricated in initial point contact. Wear 271(9–10):1719–1725
12. Li JL, Xiong DS, Dai JH, Huang ZJ, Tyagi R (2010) Effect of surface laser texture on frictional properties of nickel-based composite. Tribol Int 143:1193–1199
13. Hiraoka N, Sasaki A (1997) Effect of discontinuous hard undercoating on the life of solid film lubricant under extreme contact pressure. Tribol Int 30:429–434
14. Rahmani R, Mirzaee I, Shirvani A, Shirvani H (2010) An analytical approach for analysis and optimization of slider bearings with infinite width parallel textures. Tribol Int 43:1551–1565
15. Wang XL, Kato K, Adachi K, Aizawa K (2003) Load carrying capacity map for the surface texture design of SiC thrust bearing sliding in water. Tribol Int 36:189–197
16. Sinanoglu C (2009) Investigation of load carriage capacity of journal bearings by surface texture. Ind Lubr Tribol 61:261–270
17. Arslan A, Masjuki HH, Kalam MA (2016) Surface texture manufacturing techniques and tribological effect of surface texture on cutting tool performance: a review. Crit Rev Solid State Mater Sci 0:1–35
18. Sharma V, Pandey PM (2016) Recent advances in turning with textured cutting tools: a review. J Clean Prod 137:701–715
19. Koshy P, Tovey J (2011) Performance of electrical discharge textured cutting tools. Int J Adv Manuf Technol 60:153–156
20. Enomoto T, Sugihara T (2011) Improvement of anti-adhesive properties of cutting tool by nano/micro textures and its mechanism. Procedia Eng 19:100–105
21. Enomoto T, Sugihara T (2010) Improving anti-adhesive properties of cutting tool surfaces by nano−/micro-textures. CIRP Ann Manuf Technol 59:597–600
22. Obikawa T, Kamio A, Takaoka H, Osada A (2011) Micro-texture at the coated tool face for high performance cutting. Int J Mach Tool Manuf 51:966–972
23. Zhang K, Deng JX, Xing YQ, Li S, Gao H (2015) Effect of microscale texture on cutting performance of WC/co-based TiAlN coated tools under different lubrication conditions. Appl Surf Sci 326:107–118
24. Michielsen S, Zhang JL, Du JM, Lee HJ (2011) Gibbs free energy of liquid drops on conical fibers. Langmuir 27:11867–11872
25. Liu JL, Xia R, Li BG, Feng XQ (2007) Directional motion of droplet in a conical tube or on a conical fiber. Chin Phys Lett 24: 3210–3213
26. Radoslaw WM, Grzegorz MK, Mariusz M, Piotr N, Szymon W (2017) Structural and microhardness changes after turning of the AISI 1045 steel for minimum quantity cooling lubrication. J Mater Eng Perform 26(1):431–438
27. Lee EH, Shaffer BW (1951) The theory of plasticity applied to a problem of machining. J Appl Mech 18:405–413
28. Krolczyka GM, Marudab RW, Krolczyka JB, Nieslonya P, Wojciechowskic S, Legutko S (2018) Parametric and nonparametric description of the surface topography in the dry and MQCL cutting conditions. Measurement 121:225–239
29. Huang CH, Lee S, Sullivan JP, Chandrasekar S (2007) In situ measurement of fluid film thickness in machining. Tribol Lett 28(1):39–44
30. Wen SZ (2002) Principles of tribology, 2th edn. Tsinghua University Press, Beijing